

Received 14 August 2023, accepted 7 September 2023, date of publication 12 September 2023,
date of current version 21 September 2023.

Digital Object Identifier 10.1109/ACCESS.2023.3314588

RESEARCH ARTICLE

Research on Safety Control Method of Power Grid Energy Storage System Based on Neural Network Model

XIANGLONG CHEN¹ AND WEI XIE²

¹China Southern Power Grid Company Ltd., Guangzhou 510663, China

²College of Automation Science and Technology, South China University of Technology, Guangzhou 510641, China

Corresponding author: Xianglong Chen (chenxianglong996@163.com)

ABSTRACT This paper presents a security control method of Grid energy storage based on neural network model. The clean energy consumption effect of hybrid ESS was studied through a load forecasting method based on improved RNN (Recurrent Neural Network). Based on the current mainstream deep learning architecture, deep RNNs with different ring kernels were established to optimize the hybrid ESS model. The research results indicate that the curve obtained by this method is smoother after peak shaving and valley filling. The planned variance of this method is 43.037, which is 7.37% lower than the load variance of the literature method. It improves the stability of the distribution network operation and the absorption of photovoltaic and wind energy, reducing the cost of exceeding the limit of battery losses. The optimized operation status of microgrids can reduce costs, improve the security of microgrid systems, and better meet the proposed optimization goals.

INDEX TERMS Neural network, recurrent neural network, energy storage system, power grid.

I. INTRODUCTION

Energy is very important for human survival and development. Electric power is a clean and convenient energy source, this is of great significance to China's economic development. With the development and popularization of new energy technology, the proportion of new energy is increasing, and its ability to save ES (energy storage) is also growing. Photovoltaic power station needs to adjust its final output power through reasonable control mode, so as to realize the optimization of power generation decision and obtain the maximum long-term benefit. However, the high power input/output of large-capacity power grid ESS(energy storage system) intensifies the inconsistency of battery cells, resulting in battery capacity attenuation, which seriously affects the economy and safety of power grid ESS. In order to ensure the safety of power grid ESS, it is necessary to accurately predict the attenuation capacity of battery cells in order to carry out maintenance in advance [1], [2].

The associate editor coordinating the review of this manuscript and approving it for publication was Nurul I. Sarkar¹.

In photovoltaic microgrid, it is of great significance to configure ESS reasonably for improving the local absorptive capacity of photovoltaic and improving the economy of the system. At present, ES technology has become a research hotspot of scholars and industry at home and abroad [3], [4]. Navarro G et al. established the ESS optimal configuration model in view of the negative impact of distributed generation access to regional distribution network on load characteristics [5], taking into account ES charging and discharging power constraints, operation constraints and power flow balance constraints of distribution network. Zeinal-Kheiri S et al. chose ES battery capacity as the target, and optimized the peak regulation in real time based on dynamic programming, so as to prolong the battery life by limiting the number of charge and discharge and the depth of discharge [6]. Ouyang Jing and others put forward a new method based on online predictive control in view of the forecasting error in the process of photovoltaic power plants participating in the electricity market transaction on the same day [7]. Wang B et al. used neural network to smooth the charging and discharging process and proposed

a new bidirectional converter topology, which avoided the problems of redundancy and self-discharge of charging and discharging circuits. However, the learning process of a single neural network was unstable and the convergence speed was slow [8]. Haga H et al. studied the microgrid ES device by using fuzzy control strategy. Its control effect is only related to fuzzy control rules and membership functions of fuzzy control variables, and it has strong robustness, rapidity and adaptability [9].

The controller of ESS is an important functional unit of microgrid, and a good control strategy can effectively improve the ability of ESS to solve the negative impact on the grid when renewable energy is used in a high proportion, which is of great significance to the safe operation of microgrid. Under the background of increasing new energy permeability, accurate prediction of new energy consumption is of great significance to ensure the safe and stable operation of power grid. With the continuous progress of artificial intelligence technology, reinforcement learning is introduced into the control of power electronic system.

With the development of China's power system, the capacity of the power system is also constantly improving, and the level of informatization of the power system is also constantly improving. The collection of data from previously impossible data to current data, as well as the necessary data to further improve the accuracy of predictions, provides a theoretical basis. Deep learning, as a machine learning oriented method, has received increasing attention in recent years and has good application prospects in various fields. Therefore, conducting research on power grid load forecasting methods based on deep learning is of great significance for the development of power grid load forecasting. The main purpose of this project is to establish a neural network-based security control theory for power electronic systems based on the above research. On this basis, an improved recurrent neural network (RNN) technology is used to analyze the clean energy consumption effect of the hybrid energy storage system, and a mathematical model of the distribution network for new energy integration is constructed.

II. RESEARCH METHOD

In this paper, 40000 samples are divided as follows: there are 35000 samples in the K-Fold cross-validation set and 5000 samples in the prediction set. The cross-validation set is divided into five parts: A, B, C, D and E. The four data sets A, B, C and D are used as training sets, and E is used as validation set to get the model error. By analogy, the selected hyperparametric model is trained with the whole cross-validation set, and finally the error of the prediction set is obtained. Table 1 lists the prediction errors (MSE, RMSE, MAPE) of different models (BPNN, LSTM, GRU, CNN, Our).

A. STRUCTURE AND ANALYSIS OF HYBRID ESS

Through the hybrid ES technology, the characteristics of various ES components can be integrated, and their advantages can be complemented and maximized. Compared

with single ES element, hybrid ESS has higher power and energy density, longer service life and shorter response time [10], [11]. Because of its low cost, high technical maturity and large capacity, storage battery ES has high applicability in distributed power generation systems such as microgrid. However, the limitations of battery ES are also obvious, such as low power density, high action frequency and short service life of battery. As an important part of lithium-ion battery, solid electrolyte has the advantages of high temperature resistance, non-flammability and non-volatilization, which makes it possible for lithium-ion battery to avoid electrolyte leakage and short circuit. The equivalent circuit model of lithium ion circuit is a model constructed with basic circuit components according to its volt-ampere characteristics [12].

The capacity of storage battery refers to the amount of electric energy that storage battery can release under certain conditions. There are three ways to define the capacity of storage battery: The actual capacity refers to the maximum capacity that the battery can discharge at rated current under a certain discharge state. Nominal capacity refers to the actual capacity of the battery, which is the maximum value of the rated capacity that can be released under a certain current. Rated capacity refers to the discharge capacity of the battery under specific conditions stipulated by the state. Termination voltage value When the battery is discharged to a proper voltage value, the discharge should be terminated, which is beneficial to prolong the battery life. The size of the termination voltage will also affect the actual capacity of the battery.

Battery is an important ES device in microgrid system [13], [14]. The equivalent circuit of battery is shown in Figure 1, which is the basic model of battery and consists of internal resistance R and voltage source E in series.

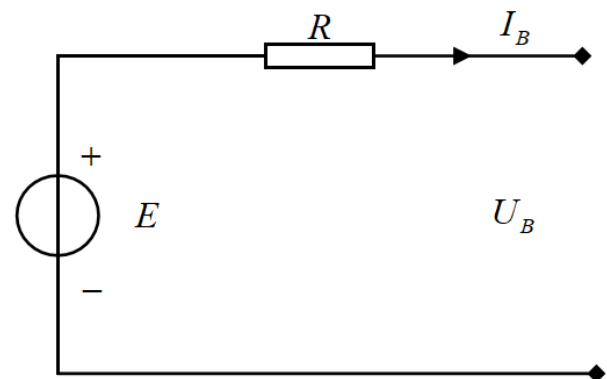


FIGURE 1. Equivalent circuit of battery basic model.

The electromotive force E is calculated by the following formula, as shown in Formula (1):

$$E = E_0 - K \frac{C_{\max}}{C_{\max} - Q_e} + A \exp(-BQ_e) \quad (1)$$

where A, B, K is the fitting parameter; C_{\max} is the maximum capacity of the battery; Q_e is the discharge capacity of the battery; E_0 is the internal potential.

The core idea of reinforcement learning method is that the controller constantly tries and tries the environment, observes the changes of the environment, obtains feedback information, and learns the optimal behavior from it, thus realizing the optimal control. In the traditional scheduling mode, the forecasting and decision-making processes are two independent stages. There is no cooperation between these two stages [15].

Optimization algorithm usually describes the uncertainty of photovoltaic power output with known probability distribution [16]. If the assumed probability distribution does not conform to the actual situation, it will affect the effectiveness of the optimization algorithm. Two independent links are merged into one link to realize the integrated scheduling of photovoltaic-ES hybrid system.

After scheduling, it is input to the photovoltaic-ES hybrid system in the power grid, and it is comprehensively scheduled according to its actual output $P_{pv,t}$ and control strategy, as shown in Figure 1. The sum of the determined ESS charging and discharging powers $P_{ESS,t}$, namely:

$$P_{sys,t} = P_{pv,t} + P_{ESS,t} \quad (2)$$

where: a positive value of $P_{ESS,t}$ indicates that ESS is in a discharging state, and a negative value indicates a charging state, that is, ESS is charged by the photovoltaic power station.

The research focus of this paper is to apply ES devices to photovoltaic-ES composite system, ES devices; Charging ES when the power price of external network is very low; When the power price of external network is high, the released power supply load. To simplify the analysis, the ES device is simplified as the following power-energy model:

$$E_{k+1} = E_k - P_k \quad (3)$$

Among them, E_k, E_{k+1} indicates that the ES equipment stores electric energy at k time and $k + 1$ time respectively, and the differences among the ES equipment are reflected in their different performance constraints, including the maximum charging and discharging power P_{max} and the maximum ES E_{max} .

Compared with battery ES, supercapacitor is complementary in function. Based on the characteristic advantages of supercapacitors, it has high applicability in power grid systems with high frequency of charging and discharging actions and high transmission power [17], [18]. The author will choose the hybrid ES scheme, integrate the performance advantages of supercapacitor and battery, improve the power density and energy density of hybrid ESS, and extend the service life of hybrid ESS. Relatively speaking, lead-acid battery has higher load capacity and lower production cost, which can reduce the use cost of hybrid ESS, thus improving the economy of hybrid ESS.

This paper systematically explores the operation mechanism of DC/DC converter. If the capacitance C and inductance L in the system are large, the switching period $[t, t + T_s]$ analysis is divided into two stages on the premise of determining the state of the device S_1 .

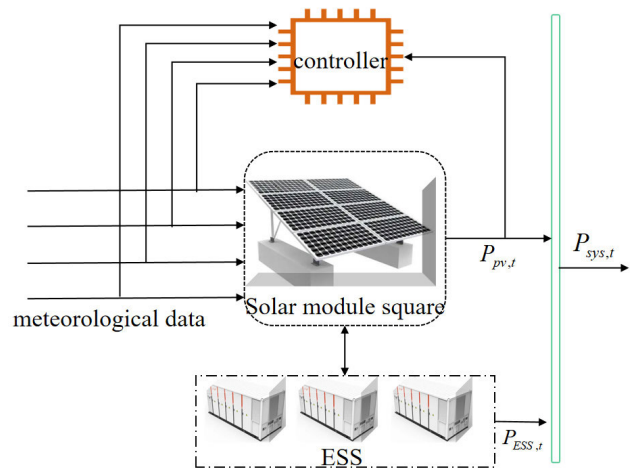


FIGURE 2. Structure of hybrid ESS.

If the device S_1 is in the on state and within the time $[t, t + DT_s]$, the range of duty ratio D is $[0, 1]$. At this time, the battery and the supercapacitor are in the charging state, and the inductor L and the capacitor C are in the electric energy storage stage. The calculation formula includes:

$$\begin{cases} L \frac{dI_c}{dt} = U_{dc} - U_c = u_{L(on)} \\ C \frac{dU_{dc}}{dt} = I_{dc} - I_c = i_{C(on)} \end{cases} \quad (4)$$

It is the goal of this paper to reduce the load rate of each line in the distribution network reasonably. Therefore, the upper limit of each line load in distribution network is a very important parameter in constructing this problem model. For the problem of insufficient line capacity in distribution network, for a fixed physical system, the maximum allowable active power flow of each line is fixed, that is, for each line, if the reference value of line capacity is given, the upper limit of line load rate can be fixed, which will not change during the whole system operation [19], [20].

We assume that the jump of the upper limit of load rate is a random process, and the probability of jump obeys a fixed distribution. At the j -th moment, the upper limit of load rate is $r(j)$, and the probability of jumping to $r(j+1)$ at the next moment is $P_{r(j)r(j+1)}$. Since the current action of the system will affect the future reward, the following infinite time discount reward function is defined:

$$\eta^v = (1 - \gamma) \lim_{U \rightarrow \infty} E \left[\sum_{u=0}^{U-1} \gamma^u f(s(j+u), a(j+u)) \right] \quad (5)$$

where γ is the discount value. The optimization goal of this paper is to reasonably schedule the energy of multiple ESS, so as to minimize the cost of the whole system in infinite time, that is to say, on the premise of meeting the power consumption of users, the number of charging and discharging is minimized, so that the load rate of distribution network can be optimized.

B. NEURAL NETWORK MODEL DESIGN OF ESS SECURITY CONTROL METHOD FOR POWER GRID

With the increasingly serious environmental problems, various distributed power generation systems based on renewable energy have been widely concerned. Micro-grid system organizes distributed power generation system, load and ESS together, this is an effective way to give full play to the efficiency of distributed power supply and improve the efficiency of electricity consumption. Compared with AC microgrid, DC microgrid can reduce energy conversion links, simplify the energy conversion process of the system, reduce system cost, reduce energy consumption and improve system security. In addition, the control of DC microgrid is simpler and the power quality is higher. In this paper, there are single flow batteries, lead-acid batteries and lithium iron phosphate batteries in the photovoltaic -ES hybrid system. In the microgrid, all ES devices are kept in a state of charge and discharge. When the ES level is low, continuous discharge will lead to over-discharge, which will seriously shorten the battery life and affect the battery performance. On the other hand, if the ES level is maintained at a high level, the battery capacity will be wasted and the efficiency will be reduced.

Neural network is abstracted or modeled after human brain or biological neural network, which has the ability of learning and simulating biological adaptability and environmental interaction. Neural network is an important product of the development of intelligent science and an important component of intelligent computing. This project will promote the in-depth development of brain and neuroscience, and the related research results will provide new ideas for solving more complex optimization problems and automation and intelligent control problems.

RNN is a special neural network. The unique signal feedback structure in RNN can correlate the current output state of the network with the previously input historical information state, and it has dynamic properties and memory ability, and can make accurate predictions [21]. The expanded RNN structure is shown in Figure 3:

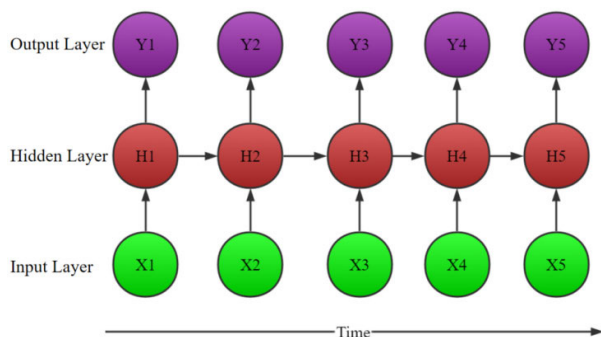


FIGURE 3. Expanded RNN structure.

RNN includes forward propagation and backward propagation. Firstly, the forward propagation is analyzed. When propagating forward, the output of the hidden layer at time t

is determined by the input at time t and the hidden layer state h_{t-1} at time $x_t, t - 1$, which can be expressed as:

$$h_t = \varphi(Ux_t + Wh_{t-1} + b) \tag{6}$$

Among them, $\varphi(\cdot)$ is the activation function, and tanh function is generally selected, and b is the bias. The output at time t is related to the state h_t of the hidden layer at time t , which can be expressed as:

$$o_t = Vh_t + c \tag{7}$$

where c represents offset. The final output of the model can be expressed as:

$$\hat{y}_t = \sigma(o_t) \tag{8}$$

Among them, σ is the activation function, and the softmax function is generally selected.

In the back propagation algorithm, the gradient of each parameter is the core of the algorithm, and the appropriate RNN model parameters are obtained by iterative gradient descent method. Although RNN has great advantages in memory and parameters, it also faces the problem of gradient disappearance, and it is difficult to process and store long time series information [22]. RNN is not only difficult to train, but also prone to gradient loss, gradient explosion and other phenomena, and faces the problem of short-term memory. The researchers found that RNN can only understand short input, but can't remember and use the information which is a little far away in a long range. This phenomenon is called short-term memory [23].

RNN can be divided into shallow RNN and deep RNN according to the network depth. Shallow network model is a data-driven adaptive algorithm, which can describe the nonlinear mapping relationship between input and output, and can mine hidden information from it [24]. For different projects and different researchers, the depth of the network can be different. Based on the current mainstream architecture of deep learning, this paper establishes the depth RNN of different loop cores to optimize the hybrid ESS model. As shown in fig. 4, it is a schematic diagram of the deep RNN architecture, and the loop kernel can be GRU(Gated Recurrent Unit) or LSTM(Long Short-Term Memory).

The deep learning network architecture in this section is built based on Keras kernel of TensorFlow2.0. The networks with different circulation modes are basically the same except for calling different high-level circulation interfaces [25], [26]. The input dimension of the network is [35,000,14,3], and there are 35,000 input vectors with the input dimension of [14,3]. Each input vector is composed of load sequence before the forecast point, load sequence of the previous day and extremely similar sequence.

The main structure of the network can be roughly divided into two major structures: cyclic structure and dimension compression. In this method, an activation function is added before the output layer, and a completely connected layer is used to connect the main structure of the whole network

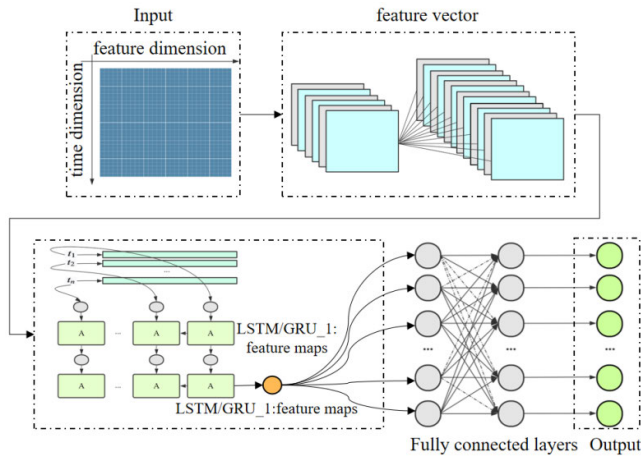


FIGURE 4. Depth RNN framework.

with the output [27]. At the same time, LSTM network can also effectively overcome the problems of unobvious gradient or abrupt change in the traditional recursive process of error transfer, and show good results in many sequential prediction tasks such as traffic, voice and handwritten words.

The LSTM unit receives the current state x_t through three different gates:

The hidden state h_{t-1} of LSTM at the last moment and the state c_{t-1} of the memory cell.

Each gate calculates the forgetting rate f_t at each moment by its logic function according to the output of the previous moment and the input of the network at that moment [28].

Finally, the state c_t of the memory cell forms the output h_t of the LSTM cell through the operation of the nonlinear function σ and the dynamic control of the output gate o_t .

$$\left. \begin{aligned} i_t &= \sigma(W_{xi}x_t + W_{hi}h_{t-1} + W_{ci}c_{t-1} + b_i) \\ f_t &= \sigma(W_{xf}x_t + W_{hf}h_{t-1} + W_{cf}c_{t-1} + b_f) \\ c_t &= f_t c_{t-1} + i_t \tanh(W_{xc}x_t + W_{hc}h_{t-1} + b_c) \\ o_t &= \sigma(W_{xo}x_t + W_{ho}h_{t-1} + W_{co}c_{t-1} + b_o) \\ h_t &= o_t \tanh(c_t) \end{aligned} \right\} \quad (9)$$

where: $W_{xc}, W_{xo}, W_{xf}, W_{xi}$ is the weight matrix connecting the input signals x_t ; $W_{hc}, W_{ho}, W_{hi}, W_{hf}$ is the weight matrix connecting the hidden layer output signal h_t ; W_{ci}, W_{cf}, W_{co} is the diagonal matrix connecting the output vector c_t of the neuron activation function and the gate function; b_i, b_f, b_c, b_o is an inherent bias vector; σ is the activation function, which is often selected as Tanh or Sigmoid.

Because GRU has obvious advantages in structure simplification, it has attracted extensive attention [29], [30]. RG(Reset Gate) is used to control the acceptance level of GRU loop structure to input vector x_t and state vector h_{t-1} at time t . The gating vector g_r is obtained by transforming the input x_t at time t and the last timestamp state h_{t-1} :

$$g_r = \sigma(W_r * [h_{t-1}, x_t] + b_r) \quad (10)$$

W_r, b_r is the parameter of RG. After random initialization, it needs to be continuously optimized and improved through

later model training. Usually, σ is set as Sigmoid activation function.

UG(Update Gate) is used to control the influence of the last timestamp state h_{t-1} and the new input h_t on the new state vector h_t . UG control vector g_z is obtained by the following formula:

$$g_z = \sigma(W_z * [h_{t-1}, x_t] + b_z) \quad (11)$$

where W_z, b_z is the parameter of UG, and σ is the activation function, and the Sigmoid function is generally used.

Under the constraints of capacity and power, the charging sequence and discharging sequence with minimum variance can make the points far away from the average value approach to the average value as much as possible, and the upper and lower limits of the peak shaving target take the adjusted sequence maximum and minimum values, which can follow the adjusted values of the sequence, and can lower the lower limit of the peak shaving target and raise the upper limit of the peak shaving target when the available capacity is exhausted.

III. RESULTS ANALYSIS AND DISCUSSION

Taking photovoltaic power generation as an example, the effectiveness of the proposed method is verified. The sampling time is 10 minutes and the sampling times are 95 times a day. The storage power plant has a battery capacity of 345MWh, a safe capacity of 30MWh and a maximum charging and discharging capacity of 15MWh. In the neural network toolbox of MATLAB, the newff function is used. The parameters of the trained BP neural network model are: the learning rate is 0.02, the maximum training times is 200, and the training accuracy is 0.001.

Fig. 5 shows the comparison of peak shaving effects of two methods under general working conditions. The curve after peak shaving and valley filling with this method is smoother. The actual load variance is 96.179, the variance after adopting the ref [5] algorithm is 46.459, and the variance after planning with this method is 43.037, which is 7.37% lower than that of the ref [5] method. Although the ref [5] algorithm prolongs the battery life, it discretizes the battery capacity, resulting in the discontinuous ES output, and the peak shaving effect is slightly worse than that of the planning control in this paper.

In order to compare and analyze the influence of users' total electricity consumption constraints on the system optimization results before and after considering the uncertainty of price-based DR (Demand response), and draw the net benefits of the system under different maximum allowable deviations of total electricity consumption before and after considering the uncertainty of price-based DR. The result is shown in Figure 6.

It can be seen that whether the uncertainty of price DR is considered or not, the net income of the system will decrease with the decrease of the maximum allowable deviation. This is mainly because with the decrease of the maximum allowable deviation, the response level of the price-based DR decreases, so the system is less affected by the uncertainty of the price-based DR. Therefore, when the maximum allowable

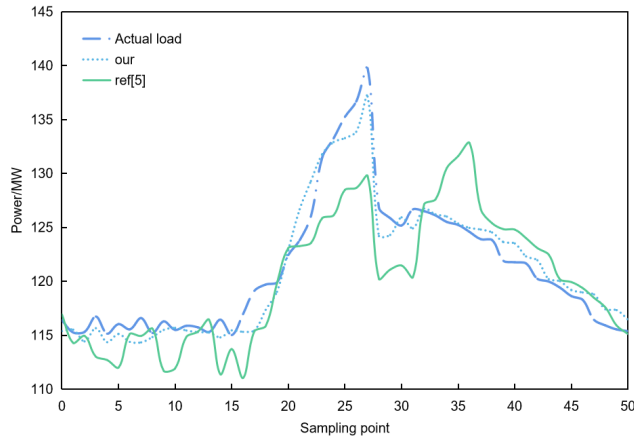


FIGURE 5. Comparison of peak shaving effect.

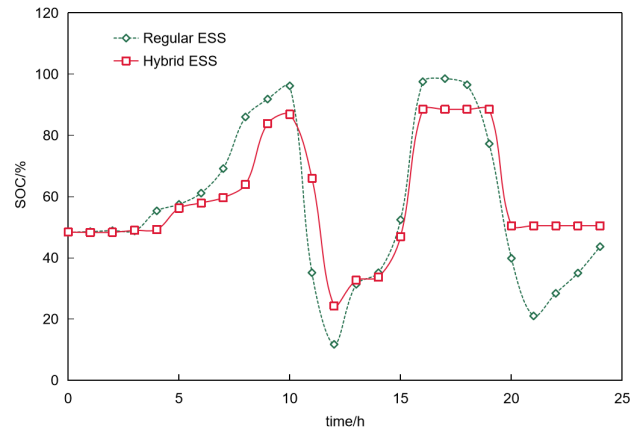


FIGURE 7. SOC of conventional ES in different scenarios.

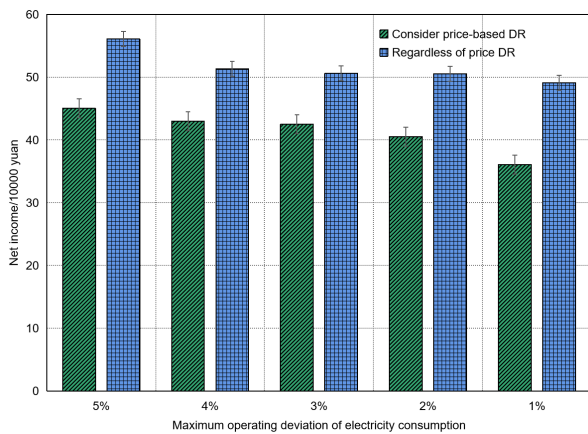


FIGURE 6. Net benefit under maximum allowable deviation.

deviation decreases, the net income gap of the system before and after considering the uncertainty also decreases.

According to the real-time system data, GRU is used to forecast, and the load demand data predicted in the day is constantly updated, and the optimal allocation is made according to the hybrid ESS proposed in this paper. The SOC(State of charge) of the hybrid ESS under different schemes is shown in Figure 7.

The research shows that the hybrid ESS can significantly absorb the active power fluctuation in the distribution network, effectively guarantee the normal operation of the traditional ES system, enhance the stability of the distribution network, absorb photovoltaic, wind power and other energy sources, reduce the ultimate loss of batteries, and improve the ESS security of the power grid.

It can be seen that after the completion of the whole scheduling period, the conventional ES SOC remains normal, thus ensuring the normal operation of the conventional ES in the hybrid ESS in the next scheduling period. However, in some scheduling cycles, the conventional ES SOC will exceed the limit, mainly because the conventional ES is deeply charged and discharged to meet the need of suppressing the fluctuation of the active power of the tie line when only

TABLE 1. Prediction error of different models.

model	MSE	RMSE	MAPE
BPNN	1.169	1.847	1.518
LSTM	2.393	1.484	0.885
GRU	1.018	1.265	0.638
CNN	1.097	2.488	0.711
Our	0.307	0.507	0.257

the conventional ES is considered. The deep learning forecasting method adopted in this paper can constantly update the forecast value of load demand, effectively improve the dispatching optimization of distribution network system, and the more accurate load forecasting results ensure the suppression of active power fluctuation of distribution network tie lines, and achieve ideal optimization results.

The 40,000 samples are divided as follows: there are 35,000 samples in the K-Fold cross-validation set and 5,000 samples in the prediction set. The cross-validation set is divided into five parts: A, B, C, D and E. The four data sets A, B, C and D are used as training sets, and E is used as validation set to get the model error. By analogy, the selected hyperparametric model is trained with the whole cross-validation set, and finally the error of the prediction set is obtained. Each model trains 45,000 samples in the cross-validation set at the optimal depth, and the prediction error results of 5,000 prediction samples in the prediction set are shown in Table 1 and Figure 8.

It can be known that GRU's MAPE (mean absolute percentage error), MSE (mean square error) and RMSE (Root Mean Squared Error) are lower than those of LSTM, and lower than those of BPNN and CNN (voluntary neural network).

IV. COMPARISON

On the whole, the combined algorithm still shows greater advantages in information extraction, and the combined prediction can achieve better results than the single algorithm.

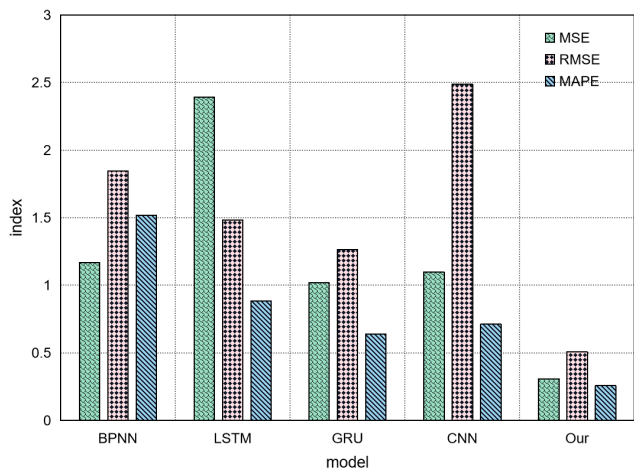


FIGURE 8. Statistical chart of prediction error of different models.

In the single algorithm prediction, RNN has a better starting point than other traditional neural network structures in time series prediction; It can also be seen that compared with other common single algorithms or similar combined algorithms, this algorithm can mine more features of time series correlation information and has better prediction accuracy.

Take the forecast results of one day as an example. See Figure 9 for the comparison of load forecast results:

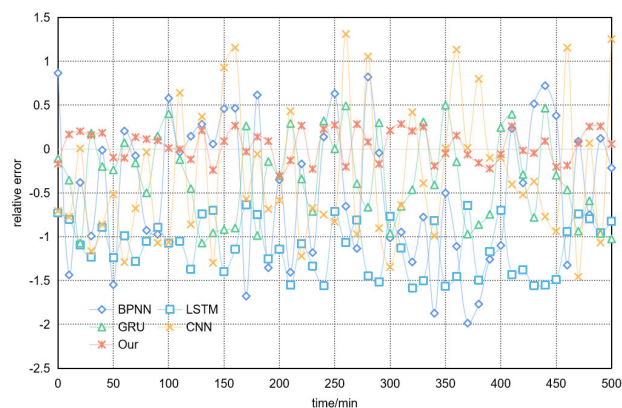


FIGURE 9. Comparison of load forecasting results.

The prediction results of GRU and LSTM are more accurate than those of CNN in terms of load change trend and specific load values, which can be attributed to the superiority of circular structure in time series analysis and prediction and the complex gate structure inside GRU and LSTM.

The prediction error of GRU model is smaller than that of LSTM, but it does not exceed the combined algorithm in this paper, and there is almost no obvious lag near the extreme point of load change, which shows that GRU has better forecasting immediacy when the load rises and falls sharply. Generally speaking, the model architecture of deep RNN and a considerable part of optimization experience are

still worth learning from other network structures when they develop into deep learning.

The optimized operation state of microgrid not only reduces the cost and improves the security in the microgrid system, but also plays a positive role in the power redistribution of the whole power system. One of the purposes of the time-of-use electricity price policy is to guide users to use electricity reasonably, that is to say, the high point of electricity price must be the high point of load, and the optimized microgrid system, for energy consumers, reducing the peak and valley prices and increasing their electricity prices can reduce the peak and valley prices, thus achieving the purpose of reducing the peak and valley. Finally, the purpose of reducing the overall energy consumption of microgrid is achieved, and the microgrid system is ensured to run smoothly, economically and reliably.

Combined with the above simulation results, it can be seen that the energy optimization control method of microgrid based on deep RNN planning method proposed in this paper has good effectiveness and reliability, and can better meet the proposed optimization objectives.

V. CONCLUSION

This paper takes a photovoltaic power station as an example to verify the effectiveness of the proposed method. The sampling interval of load data is 10 min, and the number of samples per day is 95. BP training network is established by using the newff function of neural network toolbox in MATLAB. The transfer function from input layer to hidden layer and from hidden layer to output layer are S-shaped tangent function and linear transfer function respectively. Parameters of the trained BPNN model: the learning rate is 0.02, the maximum training times is 200, and the training accuracy is 0.001.

However, due to the limitations of my conditions and time, there are still many issues that need to be improved in the process of writing the paper. If the charging and discharging efficiency of the battery is assumed to be 100%, it is not consistent with the actual charging and discharging process of the battery. In response to the energy allocation problem of multi energy storage and multi user microgrids, this project divides distributed power sources into multiple levels, regardless of differences in climate and environment. On this basis, further use techniques such as neural network dynamic programming to construct more accurate mathematical models, making them closer to real physical systems.

REFERENCES

- [1] L. Zhang, Y. Tang, S. Yang, and F. Gao, "Decoupled power control for a modular-multilevel-converter-based hybrid AC-DC grid integrated with hybrid energy storage," *IEEE Trans. Ind. Electron.*, vol. 66, no. 4, pp. 2926-2934, Apr. 2019.
- [2] J. Li, R. Xiong, H. Mu, B. Cornélusse, P. Vanderbemden, D. Ernst, and W. Yuan, "Design and real-time test of a hybrid energy storage system in the microgrid with the benefit of improving the battery lifetime," *Appl. Energy*, vol. 218, pp. 470-478, May 2018.
- [3] A. M. Joshua and K. P. Vittal, "Protection schemes for a battery energy storage system based microgrid," *Electr. Power Syst. Res.*, vol. 204, Mar. 2022, Art. no. 107701.

- [4] A. Mohammad, M. Zuhair, and I. Ashraf, "An optimal home energy management system with integration of renewable energy and energy storage with home to grid capability," *Int. J. Energy Res.*, vol. 46, no. 6, pp. 8352–8366, May 2022.
- [5] G. Navarro, M. Blanco, J. Torres, J. Nájera, Á. Santiago, M. Santos-Herran, D. Ramírez, and M. Lafoz, "Dimensioning methodology of an energy storage system based on supercapacitors for grid code compliance of a wave power plant," *Energies*, vol. 14, no. 4, p. 985, Feb. 2021.
- [6] S. Zeinal-Kheiri, S. Ghassem-Zadeh, A. M. Shotorbani, and B. Mohammadi-Ivatloo, "Real-time energy management in a microgrid with renewable generation, energy storages, flexible loads and combined heat and power units using Lyapunov optimisation," *IET Renew. Power Gener.*, vol. 14, no. 4, pp. 526–538, Mar. 2020.
- [7] O. Jing and G. Pan, "Optimal configuration strategy of energy storage system in high photovoltaic penetration micro-grid based on voltage sensitivity analysis," *High Technol. Lett.*, vol. 25, no. 3, pp. 66–74, 2019.
- [8] B. Wang, L. Xian, U. Manandhar, J. Ye, X. Zhang, H. B. Gooi, and A. Ukil, "Hybrid energy storage system using bidirectional single-microgrid multiple-port converter with model predictive control in DC microgrids," *Electr. Power Syst. Res.*, vol. 173, pp. 38–47, Aug. 2019.
- [9] H. Haga, T. Shimao, K. Kato, Y. Ito, and K. Arimatsu, "Power averaging system with multiple energy storages divided based on the amplitude of averaging power," *IEEJ Trans. Ind. Appl.*, vol. 139, no. 3, pp. 330–338, 2019.
- [10] D. Wu, D. Wang, T. Ramachandran, and J. Holladay, "A techno-economic assessment framework for hydrogen energy storage toward multiple energy delivery pathways and grid services," *Energy*, vol. 249, Jun. 2022, Art. no. 123638.
- [11] P. Patel, "Potassium batteries show promise: Hurdles remain, but potassium could someday make sense for grid storage—[news]," *IEEE Spectr.*, vol. 57, no. 3, pp. 11–12, Mar. 2020.
- [12] C. Amy, H. R. Seyf, M. A. Steiner, D. J. Friedman, and A. Henry, "Thermal energy grid storage using multi-junction photovoltaics," *Energy Environ. Sci.*, vol. 12, no. 1, pp. 334–343, 2019.
- [13] X. Yin, Y. Zhu, and J. Hu, "A sub-grid-oriented privacy-preserving microservice framework based on deep neural network for false data injection attack detection in smart grids," *IEEE Trans. Ind. Informat.*, vol. 18, no. 3, pp. 1957–1967, Mar. 2022.
- [14] L. Tian, H. Xu, and X. Zheng, "Research on fingerprint image recognition based on convolution neural network," *Int. J. Biometrics*, vol. 13, no. 1, p. 64, 2021.
- [15] F. Li, S. Fang, Y. Shen, and D. Wang, "Research on graphene/silicon pressure sensor array based on backpropagation neural network," *Electron. Lett.*, vol. 57, no. 10, pp. 419–421, May 2021.
- [16] Y. Xuan, W. Si, J. Zhu, Z. Sun, J. Zhao, M. Xu, and S. Xu, "Multi-model fusion short-term load forecasting based on random forest feature selection and hybrid neural network," *IEEE Access*, vol. 9, pp. 69002–69009, 2021.
- [17] Y. Wang, N. Zhang, and X. Chen, "A short-term residential load forecasting model based on LSTM recurrent neural network considering weather features," *Energies*, 2021, vol. 14, no. 10, p. 2737.
- [18] Y. Huang, M. Zhou, and X. Yang, "Ultra-short-term photovoltaic power forecasting of multifeature based on hybrid deep learning," *Int. J. Energy Res.*, vol. 46, no. 2, pp. 1370–1386, Feb. 2022.
- [19] J. Song, Y. Lee, and E. Hwang, "Time–frequency mask estimation based on deep neural network for flexible load disaggregation in buildings," *IEEE Trans. Smart Grid*, vol. 12, no. 4, pp. 3242–3251, Jul. 2021.
- [20] C. Shang, J. Gao, H. Liu, and F. Liu, "Short-term load forecasting based on PSO-KFCM daily load curve clustering and CNN-LSTM model," *IEEE Access*, vol. 9, pp. 50344–50357, 2021.
- [21] B. Li, Y. Liu, and L. Lai, "Computational model of grid cells based on back-propagation neural network," *Electron. Lett.*, vol. 58, no. 3, pp. 93–96, Feb. 2022.
- [22] Y. Pengfei, "Research on stock index futures arbitrage strategy based on convolutional neural network," *Adv. Appl. Math.*, vol. 10, no. 2, pp. 557–567, 2021.
- [23] Z. Ni, H. Bi, C. Jiang, H. Sun, W. Zhou, Z. Qiu, and Q. Lin, "Research on the co-pyrolysis of coal slime and cellulose based on TG-FTIR-MS, artificial neural network, and principal component analysis," *Fuel*, vol. 320, Jul. 2022, Art. no. 123960.
- [24] M. Aryanezhad, "A robust game-theoretic optimization model for battery energy storage in multi-microgrids by considering of renewable based DGS uncertainty," *Electr. Power Syst. Res.*, vol. 204, Mar. 2022, Art. no. 107591.
- [25] X. Liu, F. Zhang, Q. Sun, and W. Zhong, "Multi-objective optimization strategy of integrated electric-heat system based on energy storage situation division," *IEEE Access*, vol. 9, pp. 19004–19024, 2021.
- [26] M. Selvaraj and E. Kannan, "Enhancing power in a grid-connected system using unified power quality conditioner with black widow optimization-based floating photovoltaic system," *Int. J. Energy Res.*, vol. 46, no. 3, pp. 3095–3114, Mar. 2022.
- [27] C. Shilaja, G. Nalinashini, N. Balaji, and K. Sujatha, "Combined economic-emission dispatch of external optimization integrating renewable energy resources stochastic wind and solar," *ECS Trans.*, vol. 107, no. 1, pp. 7325–7338, Apr. 2022.
- [28] L. Tao, Y. Gao, L. Cao, and H. Zhu, "Distributed real-time pricing for smart grid considering sparse constraints and integration of distributed energy and storage devices," *COMPEL Int. J. Comput. Math. Electr. Electron. Eng.*, vol. 40, no. 5, pp. 978–996, Oct. 2021.
- [29] C. Strong, Y. Carrier, and F. Handan Tezel, "Experimental optimization of operating conditions for an open bulk-scale silica gel/water vapour adsorption energy storage system," *Appl. Energy*, vol. 312, Apr. 2022, Art. no. 118533.
- [30] S. Chen, A. Arabkoohsar, Y. Yang, T. Zhu, and M. P. Nielsen, "Multi-objective optimization of a combined cooling, heating, and power system with subcooled compressed air energy storage considering off-design characteristics," *Appl. Thermal Eng.*, vol. 187, Mar. 2021, Art. no. 116562.

• • •